

Robust Output Feedback Controller For a Class of Nonlinear Systems with Actuator Dynamics^{*}

Amgad Mohamed^{*} Mazen Alamir^{*}

^{*} Univ. Grenoble Alpes, CNRS, Grenoble INP, GIPSA-Lab, F-38400
Saint Martin D'Hères, France
(amgad.mohamed(mazen.alamir)@gipsa-lab.grenoble-inp.fr)

Abstract: This paper addresses a simple robust output feedback controller, which suits a class of nonlinear dynamical systems. It takes into account the dynamics and limitations of the actuator. This setting appears in industrial problems such as flow rate control for hydraulic turbines which is used for speed control, where controller gains tuning is important to avoid violent input signals that could excite unstable dynamics, in addition to the limitation of the actuator in use. A systematic approach is proposed to compute the parameters of a simple control law optimally to minimize the tracking error. This approach is divided into two steps. Firstly, computing bounds on some of the system's parameters and variables, then solving a nonlinear constrained optimization problem (offline). Stability analysis is carried out to guarantee that obtained parameters stabilize the system while keeping the tracking error below a certain bound. A numerical example is given to illustrate the relevance of the proposed controller.

Keywords: Robust nonlinear control, output feedback, actuator dynamics

1. INTRODUCTION

This paper addresses the problem of output feedback control design of a class of nonlinear dynamical systems, where there is a simple although uncertain relationship between the input u and the regulated output y which are linked through a subsystem's dynamics (e.g. an actuator).

The proposed controller is as simple as a PI controller, where the design process is easy to follow by practitioners. The choice of the parameters is made such that the system's asymptotic stability is guaranteed, in addition to minimizing the output tracking error. This choice also results in getting an actuator-friendly control signal, as a result of including the actuator dynamics in the analysis. This limits the excitation of unstable dynamics that lead to oscillations and/or lack of controllability.

This work extends what has been proposed in (Alamir, 2015) and (Alamir et al., 2017), where the uncertain nonlinear system is of relative degree 1, hence the control signal directly affects the regulated output dynamics (actuator dynamics are not considered). In (Alamir et al., 2017), controller parameters selection makes use of the system parameters bounds while avoiding the excitation of the uncertainties which depend on high control-derivative. This approach has been successfully applied in (Dobrowolski et al., 2017), where grid frequency is regulated by controlling the total power produced, while taking into account power transmission dynamics and uncertainties from power consumption.

Different techniques for robust output feedback design for nonlinear systems are available in the literature, there exist methods that rely on high-gain observers design, for instance, in (Yang et al., 2011), an output feedback controller is designed for a linearizable uncertain nonlinear system of relative degree n , where the nominal nonlinear model is known. A disturbance observer to estimate the disturbance and a high-gain observer to estimate the internal states are designed and the resulting controller is implemented as an output feedback. Moreover, in (Mahmoud and Zribi, 2003) an output feedback controller is proposed for uncertain nonlinear systems in addition to possibly nonlinear actuator dynamics, where a high-gain observer is used with output feedback controller under semiglobal stabilization conditions to stabilize the origin.

However, our focus is on systems where internal states reconstruction is not possible via observer design, whether due to the lack of observability, or the difficulty of the design (tight mathematical models of complex behaviors of the system are needed), or the implementation (computationally expensive).

There exist different controllers that avoid the use of observers. For instance, in (Mizumoto and Takagi, 2014) an adaptive PID is designed based on the passivity assumption of the discrete-time nonlinear system, where a neural network is used to improve the controller performance. However, in addition to the smoothness assumption of the nonlinear functions (which is not required in our approach, as it is based on the bounds of the nonlinear function), the actuator restrictions are not taken into account. Moreover, the analysis presented might not be easy to follow by practitioners due to the use of neural networks, and the

^{*} This work is funded by INNOV-Hydro Project

lack of an example that shows how the different parameters of the controller are computed.

Furthermore, (Fliess and Join, 2013) propose another technique where observer design is not required. Authors consider nonlinear systems with relative degrees (≥ 1), where they proposed an intelligent PID controller. The control signal depends on a local estimation of a nonlinear term, in addition to the PID gains, which are chosen to achieve local stability as shown in (Fliess and Join, 2014). This approach has been implemented successfully to a number of applications for example: (Join et al., 2017), (Michel et al., 2010) and (Bara et al., 2017). However, the effect of the actuator limitations, for example: saturation limits on control input signal, on the local estimation and stability is not studied. Even though actuator saturation limits are included in (Michel et al., 2010), (Tebbane et al., 2016), (Abouaïssa et al., 2017) and (Join et al., 2010), but their effects were not clearly addressed. In addition, PID tuning method proposed in (Fliess and Join, 2014) results in local asymptotic stability, however its effect on minimizing the steady-state tracking error is not addressed.

This paper is organized as follows: section 2 states the problem to be tackled in this paper. The working assumptions in section 3. The main results regarding the feasibility bounds of the control parameters and bounds on the tracking error is given in section 4. An illustrative example is given in section 5. Finally, section 6 concludes the paper and discusses possible further work.

2. PROBLEM FORMULATION

Let us consider the dynamical system given by:

$$\dot{y}(t) = \alpha(t) [q_1(t) - h(t)] \quad (1)$$

$$\dot{q}(t) = G(q(t), u(t)) \quad (2)$$

where $q \in \mathbb{R}^{n_z}$ is the internal state vector of a subsystem (e.g. an actuator) in which q_1 without loss of generality is assumed to be the variable in q which affects the dynamics of the regulated variable $y \in \mathbb{R}$ while $u \in [u_{min}, u_{max}]$ is the directly manipulated variable. $G(q, u)$ is possibly an unknown map that could have non-linearities (e.g. saturation), however it is necessary to be able to identify bounds on the behavior of $G(q, u)$ as shown in section 3. Moreover, $h(t) \in [h_{min}, h_{max}]$ is an unknown term which could be nonlinear with known bounds h_{min} and h_{max} . Finally, $\alpha(t) \in [\underline{\alpha}, \bar{\alpha}]$ is an unknown positive scalar term that might be time-varying, with known bounds $\underline{\alpha}$ and $\bar{\alpha}$.

In this paper, the following simple output feedback control law is considered:

$$u = S(\lambda(y_d - y) + z) \quad (3)$$

$$\dot{z} = \lambda_f(u - z) \quad (4)$$

Where y_d is a constant set-point for the regulated output y , $\lambda, \lambda_f > 0$ are the controller gains and the function S is defined as follows:

$$S(v) := \begin{cases} v_{max} & \text{if } v \geq v_{max} \\ v_{min} & \text{if } v \leq v_{min} \\ v & \text{otherwise} \end{cases} \quad (5)$$

where $v \in [v_{min}, v_{max}]$

The standard form given by (1)-(2) that includes uncertain and nonlinear terms possibly makes it difficult to design observers to estimate the internal states of the system which are needed for more advanced control design, thus robust output feedback is a good choice in that case. The simple control law considered in (3)-(4) is preferred for industrial applications due to its simple requirements and implementation. The standard form given (1)-(2) is quite generic, thus it is compatible with existing systems, especially if (2) is considered to model the actuator dynamics.

A system that we are interested in applying the control law (3)-(4) to is water flow rate (Q) control for hydraulic turbines to be used for the turbine's rotational speed control, where u is the guide vane opening set-point that is sent to the actuator that gives the guide vane opening (q_1) that directly affects Q at the turbine. Also note that, Q depends on nonlinear uncertain relationships describing the turbine's dynamics called 'Hill Charts'. Moreover, the simplicity of the considered control law is highly encouraged by companies working in that domain which is compatible with existing platforms. Furthermore, careful selection of the controller gains (λ, λ_f) plays an important role in this application, since high control gains could excite sharp oscillations at the turbine as shown in Zuo et al. (2016) which is not desirable. Finally, the actuator currently used imposes different saturation bounds on the rate of change of the guide vane opening, so a careful choice of the controller gains is required to make sure we do not ask the actuator much more than what it could provide.

Another application where the controller could be used is speed control for hybrid electric vehicles (HEV) that makes use of DC motors. In such systems as explained in Kumar et al. (2016) the actuator is the electronic throttle which accepts armature voltage as an input and outputs angular throttle position which is then used to control vehicle speed. Uncertainty is an important feature of such systems while friction terms are usually nonlinear which show up in the dynamical equation of the speed of the vehicle.

Thus, in the following sections, a systematic way to obtain a pair (λ, λ_f) that gives a convenient closed-loop behavior of the system will be discussed, in addition to an assessment criteria based on which these controller gains are selected will be detailed. This helps applying this control law to different systems that could be put in the standard form (1)-(2).

3. WORKING ASSUMPTIONS

In this section, assumptions on the system's uncertain parameters and variables as introduced, which limits the class of unknown dynamics for which a pair (λ, λ_f) exists that results in an appropriate behavior of the control law (3)-(4).

In order to show the importance of these assumptions and for the analysis to be carried out in the forthcoming section, equation (3) needs to be put in a different form as follows:

$$\dot{y} = \alpha [q_1 - h] \quad (6)$$

$$= \alpha [u - h'] \quad \text{with} \quad h' := h + (u - q_1) \quad (7)$$

The first crucial assumption which guarantees controllability is that u can ultimately dominate the partially unknown term $h \in [h_{min}, h_{max}]$ with some margins, denoted by $\varrho_- > 0$ and ϱ_+ , in other words the bounds of h are contained within the bounds of u . This guarantees that the sign of \dot{y} can ultimately be changed by changing u , hence obtaining a bounded tracking error.

Assumption 1. (u dominates h). There exists two scalars $\varrho_- > 0$ and $\varrho_+ > 0$ such that:

$$u_{max} \geq h_{max} + \varrho_+ \quad ; \quad u_{min} \leq h_{min} - \varrho_- \quad (8)$$

Next, we assume that the dynamics of the subsystem G to be referred to by 'actuator' given by (2) satisfy the following natural assumption which simply states that the tracking error on the actuator output q_1 decreases with the bandwidth of the reference signal:

Assumption 2. (Assumption on the actuator).

For any reference signal u on q_1 and $\rho > 0$ such that:

$$|\dot{u}| \leq \rho \quad (9)$$

there exist positive reals $\sigma, \pi_1 > 0$ such that the following properties hold **after a finite time**.

$$|u(t) - q_1(t)| \leq \sigma \rho \quad (10)$$

$$|\dot{u}(t) - \dot{q}_1(t)| \leq \pi_1 \rho \quad (11)$$

This assumption as will be shown in the next section, simply states that the slower is the reference trajectory $u(\cdot)$ (the smaller is ρ), the smaller is the tracking errors $|u(t) - q_1(t)|$ and $|\dot{u}(t) - \dot{q}_1(t)|$.

The chosen values of σ and π_1 could be sufficiently high to ensure the satisfaction of this assumption, however choosing values which are too high would result in a more conservative choice of the controller's parameters.

It is important to note that σ and π_1 are obtained offline, thus a clean input signal u could be used and the output signal q_1 could be filtered to avoid sharp oscillations of \dot{u} and \dot{q}_1 . Moreover, making use of the knowledge of the nature of the actuator in use (e.g. using identified models), clean q_1 signals could be acquired.

4. SUFFICIENT CONDITIONS ON CONTROL PARAMETERS AND BOUNDS ON THE TRACKING ERROR

In this section, the properties of the parameters (λ, λ_f) of the control law (3)-(4) which result in the desired closed-loop behavior are introduced. This is achieved by utilizing upper and lower bounds of the system's parameters.

We begin by deriving upper and lower bounds on h' , needed in this section, by combining Assumptions 1 and 2, in addition to the definition of h' in (7) to get:

$$h'_{max} := h_{max} + \sigma \rho \quad (12)$$

$$h'_{min} := h_{min} - \sigma \rho \quad (13)$$

Lemma 1. Under the control law (3)-(4), for all $\lambda > 0$ satisfying:

$$\lambda < \frac{1}{\bar{\alpha}\sigma} \quad (14)$$

the following inequality holds:

$$|\dot{u}| \leq \rho := \frac{\lambda}{1 - \lambda \bar{\alpha}\sigma} \left[\bar{\alpha}\bar{\varrho} + \frac{\lambda_f}{\lambda} \Delta_u \right] \quad (15)$$

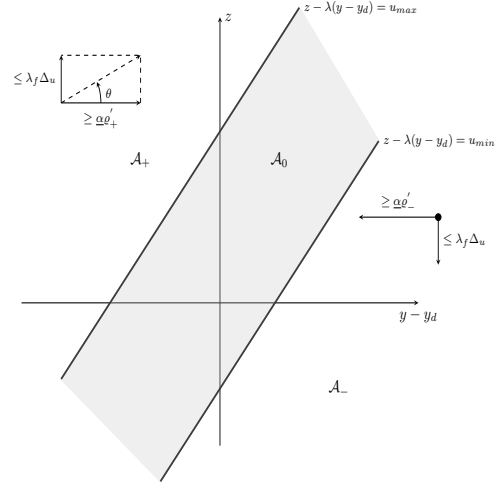


Fig. 1. Definition of the three regions \mathcal{A}_0 , \mathcal{A}_+ and \mathcal{A}_- used in the analysis of the stability of the closed-loop system with the proposed feedback law.

where

$$\Delta_u := u_{max} - u_{min} \quad (16)$$

$$\bar{\varrho} := \max\{u_{max} - h_{min}, h_{max} - u_{min}\} \quad (17)$$

PROOF. Note first of all that by the very definition of u , namely:

$$u = S(\lambda(y_d - y) + z)$$

one can write:

$$|\dot{u}| \leq \lambda|\dot{y}| + |\dot{z}| \leq \lambda|\dot{y}| + \lambda_f \Delta_u \quad (18)$$

and since

$$\dot{y} = \alpha(u - (h + (u - q_1)))$$

one can write for any ρ such that $|\dot{u}| \leq \rho$ [thanks to (9) of Assumption 2]:

$$|\dot{y}| \leq \bar{\alpha}(\bar{\varrho} + \sigma\rho)$$

and injecting this in (18) leads to the following inequality that holds for any upper bound ρ on the evolution of $|\dot{u}|$:

$$|\dot{u}| \leq \lambda[\bar{\alpha}(\bar{\varrho} + \sigma\rho)] + \lambda_f \Delta_u \leq \rho$$

Therefore, the bound ρ we are looking for must satisfy the inequality:

$$\rho \geq \lambda[\bar{\alpha}(\bar{\varrho} + \sigma\rho)] + \lambda_f \Delta_u$$

Which gives (15), thanks to (14), this obviously ends the proof. \square

Going further in the analysis of the closed-loop behavior, the following sets are defined as shown in Figure 1:

$$\mathcal{A}_+ := \{(y, z) \mid z - \lambda(y - y_d) \geq u_{max}\} \quad (19)$$

$$\mathcal{A}_- := \{(y, z) \mid z - \lambda(y - y_d) \leq u_{min}\} \quad (20)$$

$$\mathcal{A}_0 := \{(y, z) \mid z - \lambda(y - y_d) \in (u_{min}, u_{max})\} \quad (21)$$

Note that by definition, if $(y, z) \in \mathcal{A}_+$ then $u = u_{max}$ and if $(y, z) \in \mathcal{A}_-$ then $u = u_{min}$. While if $(y, z) \in \mathcal{A}_0$ then the control input is not saturated, in other words $u = \lambda(y_d - y) + z$.

Before proceeding, ϱ'_+ and ϱ'_- needed for the upcoming results, are defined as follows:

$$\varrho'_+ := u_{max} - h_{max} - \sigma\rho > 0 \quad (22)$$

$$\varrho'_- := h_{min} - \sigma\rho - u_{min} > 0 \quad (23)$$

Based on these definitions, the following result can be obtained:

Lemma 2. (\mathcal{A}_0 is attractive and invariant)

If $0 < \lambda < \frac{1}{\alpha\sigma}$ and λ_f are such that:

$$\lambda_f < \varphi(\lambda, \lambda_f) \quad (24)$$

where

$$\varphi(\lambda, \lambda_f) := \left[\min \left\{ \frac{\min\{\varrho'_+(\lambda, \lambda_f), \varrho'_-(\lambda, \lambda_f)\}}{\Delta_u}, \frac{1}{4} \right\} \right] \times \frac{\alpha\lambda}{\alpha\sigma}$$

Then the set \mathcal{A}_0 is attractive and invariant for the closed-loop dynamics resulting from the control law (3)-(4) and for any constant desired value y_d .

PROOF OF ATTRACTIVITY OF \mathcal{A}_0 . If for any $0 < \lambda < \frac{1}{\alpha\sigma}$ used in (3)-(4), λ_f satisfies the following inequality:

$$\lambda_f < \frac{\alpha\varrho'_+}{\Delta_u} \lambda \quad (25)$$

Then, the set \mathcal{A}_0 is attractive for all initial state such that $(y - y_d, z) \in \mathcal{A}_+$. This can be proved if one can prove that the angle θ depicted in Figure 1 is lower than $\arctan(\lambda)$ which leads to $\dot{z} < \lambda\dot{y}$ (see Figure 1). Using (7) in addition to the condition (22) together with the fact that z necessarily belongs to $[u_{min}, u_{max}]$ enable to write:

$$\tan \theta \leq \frac{\lambda_f \Delta_u}{\alpha\varrho'_+} \quad (26)$$

which obviously gives the result. \square

Using the same arguments for any $0 < \lambda < \frac{1}{\alpha\sigma}$ used in (3)-(4) in addition to condition (23), if λ_f satisfies the following inequality:

$$\lambda_f < \frac{\alpha\varrho'_-}{\Delta_u} \lambda \quad (27)$$

then the set \mathcal{A}_0 is attractive for all initial state such that $(y - y_d, z) \in \mathcal{A}_-$. Δ

PROOF OF INVARIANCE OF \mathcal{A}_0 . The invariance results from the simple fact that when the state approaches the boundaries of \mathcal{A}_0 with any of \mathcal{A}_+ or \mathcal{A}_- , it is repulsed back before reaching the boundary whenever the requirements of Lemmas 1 and 2 hold. This is precisely implied by the following condition for any $0 < \lambda < \frac{1}{\alpha\sigma}$:

$$\lambda_f < \frac{\alpha \min\{\varrho'_+, \varrho'_-\}}{\Delta_u} \lambda \quad (28)$$

This proves that \mathcal{A}_0 is globally attractive and invariant. Δ

The only thing that remains to be analyzed regarding the stability of the closed-loop behavior, is related to the behavior of the closed-loop system inside the region \mathcal{A}_0 described by:

$$\begin{bmatrix} \dot{y} \\ \dot{z} \end{bmatrix} = \begin{bmatrix} -\alpha\lambda & \alpha \\ -\lambda_f\lambda & 0 \end{bmatrix} \begin{bmatrix} y - y_d \\ z - h' \end{bmatrix} \quad (29)$$

The behavior when inside \mathcal{A}_0 , can be proved to be stable by showing that poles of the dynamical system (29) have

negative real parts. This enables the following result to be established.

If for a given $0 < \lambda < \frac{1}{\alpha\sigma}$, we get the following:

$$\lambda_f = r \times \frac{\alpha\lambda}{4} \quad ; \quad r \in (0, 1) \quad (30)$$

then the matrix:

$$A_0 := \begin{bmatrix} -\alpha\lambda & \alpha \\ -\lambda_f\lambda & 0 \end{bmatrix}$$

possesses two real and strictly negative eigenvalues $p_{1,2}$. More precisely:

$$p_{1,2} = -\frac{\alpha\lambda}{2} [1 \pm \sqrt{1-r}] \quad (31)$$

Combining (28) and (30) proves Lemma 2 Δ

The previous results lead to the following Proposition:

Proposition 3. (Main Result of the Paper). Under the assumptions of Lemmas 1 and 2, if the pair (λ, λ_f) is chosen such that the following inequalities are satisfied for some $\beta \in (0, 1)$:

$$\lambda \leq \frac{\beta}{\sigma\alpha} \quad ; \quad \lambda_f \leq \beta\varphi(\lambda, \lambda_f) \quad (32)$$

Then, the following property holds regarding the tracking error for a constant y_d :

$$\lim_{t \rightarrow \infty} |y_d - y(t)| = \frac{\delta + \pi_1 \rho(\lambda, \lambda_f)}{\lambda\lambda_f} \quad (33)$$

where $|\dot{h}| \leq \delta$

PROOF OF FEASIBILITY OF (32). The existence of (λ, λ_f) pairs satisfying the constraints (32) is guaranteed, due to the fact that $\rho(0, 0) = 0$ meaning that for sufficiently small (λ, λ_f) , $\varrho'_+(\lambda, \lambda_f) > 0$ and $\varrho'_-(\lambda, \lambda_f) > 0$ and hence, the right hand side of (24) is strictly positive. Δ

PROOF OF (33). Since, the set \mathcal{A}_0 is proven to be globally attractive by Lemma 2, the dynamics defined by (29) prevails after a finite time t_0 . Therefore, one has for all $t \geq t_0$:

$$\begin{bmatrix} e_y(t) \\ e_z(t) \end{bmatrix} = e^{A_0(t-t_0)} \begin{bmatrix} e_y(t_0) \\ e_z(t_0) \end{bmatrix} - \int_{t_0}^t e^{A_0(t-\tau)} \begin{bmatrix} 0 \\ \dot{h}'(\tau) \end{bmatrix} d\tau$$

where $\begin{bmatrix} e_y(t) \\ e_z(t) \end{bmatrix} = \begin{bmatrix} y - y_d \\ z - h' \end{bmatrix}$ and since Lemma 2 makes A_0 Hurwitz invertible, the last expression asymptotically behaves like:

$$A_0^{-1} \begin{bmatrix} 0 \\ \max_{\tau \in [t_0, t]} |\dot{h}'(\tau)| \end{bmatrix} = \begin{bmatrix} -\frac{1}{\lambda\lambda_f} \\ -\frac{1}{\lambda_f} \end{bmatrix} \max_{\tau \in [t_0, t]} |\dot{h}'(\tau)|$$

By using:

$$\max_{\tau \in [t_0, t]} |\dot{h}'(\tau)| = \delta + \pi_1 \rho$$

we obviously end up with the result in (33). Δ

Hence, for a given actuator dynamical system and bounds on the system's variables, the controller gains (λ, λ_f) can be selected by solving the following optimization problem:

$$(\lambda, \lambda_f) \leftarrow \arg \min_{(\lambda, \lambda_f)} \left[\frac{\delta + \pi_1 \rho(\lambda, \lambda_f)}{\lambda \lambda_f} \right] \quad (34)$$

$$\text{under the constraints} \begin{cases} 0 \leq \lambda \leq \frac{\beta}{\sigma \bar{\alpha}} \\ 0 \leq \lambda_f \leq \beta \varphi(\lambda, \lambda_f) \\ 0 \leq \rho(\lambda, \lambda_f) \leq \rho_\ell \end{cases} \quad (35)$$

It can be viewed as a way of determining the *combined gains*, that is compatible with the stability requirement (represented by the first two constraints in (35)), and minimizes the upper bound on the asymptotic tracking error given by (34). This is achieved while keeping ρ below a certain value ρ_ℓ (represented by the last constraint in (35)), where ρ_ℓ to be chosen or imposed by the actuator's limitation.

5. ILLUSTRATIVE EXAMPLE

Let us consider the following system:

$$\dot{y} = \alpha [q_1 - h(t)] \quad (36)$$

The unknown signal $h(t)$ is given by:

$$h(t) = 5 - 1.1 \cos(1.2t) - 0.4 \sin(2t + \pi/6) \quad (37)$$

Therefore, the bounds $\underline{h} = 3.5$, $\bar{h} = 6.5$ and $\delta = 2.2$. Moreover, $\underline{\alpha} = 0.8$ and $\bar{\alpha} = 1.2$ are chosen where $\alpha = 1$.

The actuator in use is given by:

$$\dot{x}_a = AS(x_a) + Bu \quad ; \quad q_1 = Cx_a \quad (38)$$

where A , B , C and x_a are given by:

$$A = \begin{bmatrix} 0 & 1 \\ -50 & -10 \end{bmatrix}; B = \begin{bmatrix} 0 \\ 50 \end{bmatrix}; C = [1 \ 0]; x_a = \begin{bmatrix} q_1 \\ \dot{q}_1 \end{bmatrix}$$

It can be noticed that actuator's internal states have saturation limits $S(x_a)$ defined in (5) for each element of x_a , which introduces a nonlinearity in the actuator's dynamics. To be more specific, we have $S(q_1)$, where $q_1 \in [0, 10]$, in addition we have $S(\dot{q}_1)$, where $\dot{q}_1 \in [-60, 60]$. The saturation bounds of u are $u_{min} = 0$ and $u_{max} = 10$.

The control objective is for y to track a set-point $y_d = 50$

5.1 Identification of σ and π_1

The identification of σ and π_1 is done by using an input signal $u = u_i$ given by (39), where (38) is used to compute q_1 . The differences $|u_i - q_1|$ and $|\dot{u}_i - \dot{q}_1|$ are computed, afterwards (10)-(11) are used to compute σ and π_1 , where an upper bound on the allowable rate of change of the control input ρ is chosen to be equal to maximum possible $|\dot{q}_1|$, namely $\rho_\ell = 60$.

The selection of the identification signal is based on the need to have $y = y_d$ at steady state, to achieve this, u_i is set to u_{max} for t_s seconds, then oscillates in a way that mimics h making use of the available knowledge of h . Thus, the identification input signal used is a piece-wise function given by:

$$u_i := \begin{cases} u_{max} & \text{if } t \leq t_s \\ c_0 + c_1 \cos(c_2 t) & \text{otherwise} \end{cases} \quad (39)$$

where $t_s = 10$ and c_0 , c_1 and c_2 are computed recursively as shown in Algorithm 1.

Algorithm 1 Actuator Bounds Identification

```

1:  $\pi_1 \leftarrow 0$  ;  $\sigma \leftarrow 0$ 
2: while  $k < 200$  do
3:    $s_+ \leftarrow h_{max} + \sigma \rho_\ell$  ;  $s_- \leftarrow h_{min} - \sigma \rho_\ell$ 
4:    $c_0 \leftarrow (s_+ + s_-)/2$ 
5:    $c_1 \leftarrow (s_+ - s_-)/2$ 
6:    $c_2 \leftarrow (\delta + \pi_1 \rho_\ell)/c_1$ 
7:    $u_i \leftarrow \text{identsignal}(u_{max}, c_0, c_1, c_2)$ 
8:    $q_1 \leftarrow \text{actuator}(u_i)$ 
9:   Compute  $\dot{u}_i$  and  $\dot{q}_1$ 
10:   $\sigma \leftarrow |u_i - q_1|/\rho_\ell$  ;  $\pi_1 \leftarrow |\dot{u}_i - \dot{q}_1|/\rho_\ell$ 
11:   $k \leftarrow k + 1$ 
12: end while
13: return  $\sigma, \pi_1$ 

```

Thus we get:

$$\sigma = 0.0107 \quad ; \quad \pi_1 = 0.0152$$

5.2 Optimal Pair (λ, λ_f) Computation

We can solve the nonlinear constrained optimization problem given by (34)-(35) (shown in Figure 2) for $\beta = 0.99$, to obtain (λ, λ_f) that minimizes the upper bound on the tracking error, while satisfying the stability constraints, thus we get:

$$\lambda = 5.6 \quad ; \quad \lambda_f = 1.1 \quad ; \quad \lim_{t \rightarrow \infty} |y_d - y(t)| = 0.5$$

Figure 3 shows the closed-loop simulation when using the optimal values of (λ, λ_f) , and as shown a good tracking performance is achieved after finite time where the tracking error is less than 0.3. As expected after finite time the difference between u and q_1 respects it's upper bound, resulting in h' to respect it's bounds.

On the other hand, when using $\lambda = 10$ and $\lambda_f = 1.1$, we get the closed-loop simulation results shown in Figure 4, higher tracking error can be observed, furthermore a more vigorous control input signal when compared to that from Figure 3. This shows the proposed approach of computing an optimal pair (λ, λ_f) by defining the bounds of the system's parameters and for a given actuator, the nonlinear constrained optimization problem (34)-(35) can be solved which results in a satisfying behavior.

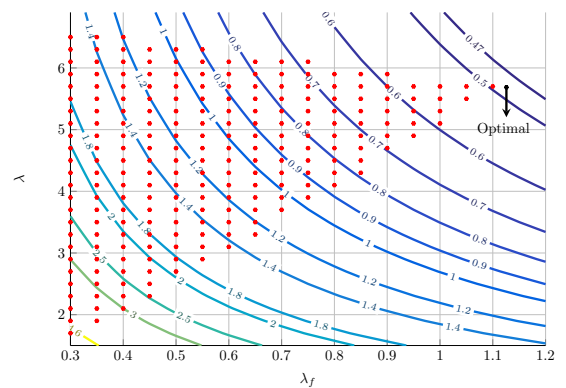


Fig. 2. Contour plot of the cost function (34), where dots are the feasible solutions of the cost function, while the optimal solution is indicated

6. CONCLUSION AND FUTURE WORK

In this paper, the problem of output feedback control of a class of uncertain nonlinear systems, in addition to a

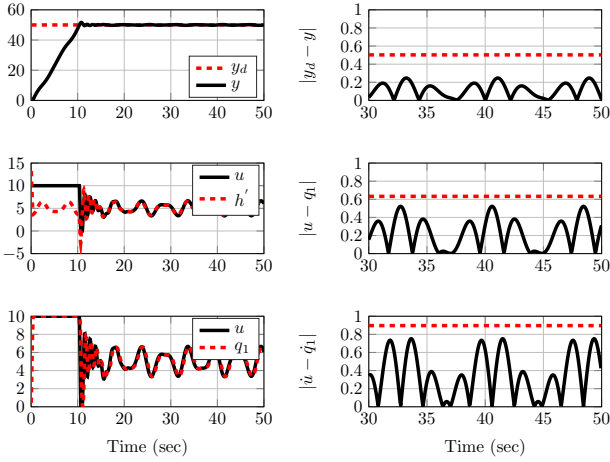


Fig. 3. Closed loop simulation results for $\lambda = 5.6$ and $\lambda_f = 1.1$ (optimal solution), where red dotted lines on plots on the right side represent upper bounds computed by (33),(10) and (11) respectively.

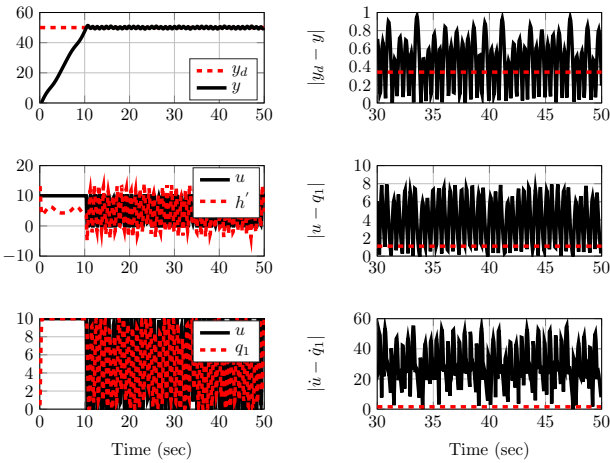


Fig. 4. Closed loop simulation results for $\lambda = 10$ and $\lambda_f = 1.1$, where red dotted lines on plots on the right side represent upper bounds computed by (33),(10) and (11) respectively.

subsystem's dynamics, namely in our case is the actuator's dynamical equation is analyzed. An approach to obtain the the gains of the simple control law is proposed. This approach involves two steps procedure:

- (1) Obtain the required bounds on some of the system's parameters and variables using simulations or system identification
- (2) Solve a nonlinear constrained optimization problem (offline) to obtain the controller gains which are guaranteed to give a converging tracking error that respects an upper bound after finite time.

The next step would be to apply this controller on speed control of hydraulic turbines where actuator dynamics play an important role as briefly explained in this paper.

REFERENCES

Abouaïssa, H., Fliess, M., and Join, C. (2017). On ramp metering: Towards a better understanding of alinea via model-free control. *International Journal of Control*, 90(5), 1018–1026.

Alamir, M. (2015). On Controlling Unknown Scalar Systems with Low Gain Feedback. Research report, GIPSA-lab. URL <https://hal.archives-ouvertes.fr/hal-01215808>. Rapport interne de GIPSA-lab.

Alamir, M., Dobrowolski, J., and Mohamed, A.T. (2017). Output Feedback Control of a Class of Uncertain Systems Under Control-derivative dependent disturbances. In *20th IFAC World Congress (IFAC WC 2017)*. Toulouse, France.

Bara, O., Olama, M., Djouadi, S., Kuruganti, T., Fliess, M., and Join, C. (2017). Model-free load control for high penetration of solar photovoltaic generation. *arXiv preprint arXiv:1707.02518*.

Dobrowolski, J., Alamir, M., Bacha, S., Gualino, D., and Wang, M.X. (2017). On higher order dynamics in the fundamental equation of frequency in islanded microgrids. In *20th IFAC World Congress (IFAC WC 2017)*, Proceedings of the IFAC World Congress. Toulouse, France.

Fliess, M. and Join, C. (2013). Model-free control. *International Journal of Control*, 86(12), 2228–2252.

Fliess, M. and Join, C. (2014). Stability margins and model-free control: A first look. In *Control Conference (ECC), 2014 European*, 454–459. IEEE.

Join, C., Bernier, J., Mottelet, S., Fliess, M., Rechdaoui-Guérin, S., Azimi, S., and Rocher, V. (2017). A simple and efficient feedback control strategy for wastewater denitrification. *arXiv preprint arXiv:1703.05278*.

Join, C., Robert, G., and Fliess, M. (2010). Vers une commande sans modèle pour aménagements hydroélectriques en cascade. *arXiv preprint arXiv:1003.0664*.

Kumar, V., Rana, K., and Mishra, P. (2016). Robust speed control of hybrid electric vehicle using fractional order fuzzy pd and pi controllers in cascade control loop. *Journal of the Franklin Institute*, 353(8), 1713–1741.

Mahmoud, M.S. and Zribi, M. (2003). Robust output feedback control for nonlinear systems including actuators. *Systems Analysis Modelling Simulation*, 43(6), 771–792.

Michel, L., Join, C., Fliess, M., Sicard, P., and Chériti, A. (2010). Model-free control of dc/dc converters. In *Control and Modeling for Power Electronics (COMPEL), 2010 IEEE 12th Workshop on*, 1–8. IEEE.

Mizumoto, I. and Takagi, T. (2014). Output tracking control of discrete-time nonlinear systems by adaptive pid based on output feedback passivity. In *Intelligent Control and Automation (WCICA), 2014 11th World Congress on*, 2584–2589. IEEE.

Tebbani, S., Titica, M., Join, C., Fliess, M., and Dumur, D. (2016). Model-based versus model-free control designs for improving microalgae growth in a closed photobioreactor: Some preliminary comparisons. In *Control and Automation (MED), 2016 24th Mediterranean Conference on*, 683–688. IEEE.

Yang, Z.J., Hara, S., Kanae, S., and Wada, K. (2011). Robust output feedback control of a class of nonlinear systems using a disturbance observer. *IEEE Transactions on Control Systems Technology*, 19(2), 256–268.

Zuo, Z., Fan, H., Liu, S., and Wu, Y. (2016). S-shaped characteristics on the performance curves of pump-turbines in turbine mode—A review. *Renewable and Sustainable Energy Reviews*, 60, 836–851.